Biomass, microbial composition and functions are responsible for the differential removal of trace organic chemicals in biofiltration systems

Lijia Cao [a], David Wolff [b], Renato Liguori [a, c], Christian Wurzbacher [a, *], Arne Wick [b]

[a] *Chair of Urban Water Systems Engineering, Technical University of Munich, Am Coulombwall 3, 85748 Garching, Germany*

[b] *Federal Institute of Hydrology (BfG), 56068 Koblenz, Am Mainzer Tor 1, Germany*

[c] *Department of Science and Technology, Parthenope University of Naples, Centro direzionale Isola –C4, 80143, Napoli, Italy*

[*] Correspondence: christian@wurzbacher.cc

One sentence summary: The variability of global micropollutant removal performance of biofiltration sites is foremost explained by microbial biomass as ATP, however, residual variation of single compound removal rates is correlated with the biofilter's microbiome.

Abstract

Biofiltration processes help to remove trace organic chemicals (TOrCs) both in wastewater and drinking water treatment systems. However, the detailed TOrCs biotransformation mechanisms as well as the underlying drivers behind the variability of site specific transformation processes remain elusive. In this study, we used laboratory batch incubations to investigate the biotransformation of 51 TOrCs in eight bioactive filter materials of different origins treating a range of waters, from wastewater effluents to drinking water. Microscopy, 16S rRNA amplicon and whole metagenome sequencing for assessing associations between the biotransformation rate constants, microbial composition and genetic potential complemented chemical analysis. We observed strong differences in the mean global removal of TOrCs between the individual sand filters (-1.4% to 58%), which were mirrored in overall biomass, microbial community composition, and enzyme encoding genes. From the six investigated biomass markers, ATP turned out to be a major predictor of the mean global biotransformation rate, while compound specific biotransformations were correlated with the microbial community composition. High biomass ecosystems were indicated in our systems by a dominance of Nitrospirae, but individual TOrC biotransformation was statistically connected to rare taxa (< 2%) such as *Hydrogenophaga,* or indiviudal enzymes such as the enoyl-CoA hydratase/3-hydroxyacyl-CoA dehydrogenase gene. In general, this study provides new insights into so far rarely addressed variability of TOrCs biotransformation. We propose novel biological indicators for the removal performance of TOrCs in biofiltration systems, highlighting the role of ATP in

predicting and normalizing the global transformation, and the role of the microbial community for the individual transformation of TOrCs in engineered and natural systems.

Keywords: sand filters; metagenome; amplicon sequencing; micropollutants; biotransformation; water treatment; microbiome

Introduction

Trace organic chemicals (TOrCs) such as pharmaceuticals, personal care products and pesticides, have raised emerging concerns regarding their effects on the aquatic environment. These anthropogenic compounds usually enter the wastewater system, and may finally end up in the receiving water bodies, leading to their frequent detection in surface water, ground water and even drinking water at the concentration ranging from few $ng \cdot L^{-1}$ to several $\mu g \cdot L^{-1}$ (Yang *et al*. 2017; Montiel-León *et al*. 2018; Tröger *et al*. 2018). For example, the widely used artificial sweetener acesulfame has been detected worldwide in wastewater treatment plants (WWTPs) at 10 to 100 $\mu g \cdot L^{-1}$, and consequently, appears in rivers and groundwater with concentrations up to the double-digit $\mu g \cdot L^{-1}$ range (Castronovo *et al*. 2017). The effects of residual TOrCs on aquatic ecosystems and the human health have been studied in recent years. For example, Shao *et al*. (2019) found that ten micropollutants with concentrations from 1.1 to 14.4 $mg \cdot L^{-1}$ caused toxicity on zebrafish embryos, aquatic invertebrates and algae. However, there are few examples showing toxic effects also in the sub $mg \cdot L^{-1}$ range for personal care products, hormones, antibiotics, biocides and pesticides (Vieno *et al*. 2014; Yang *et al*. 2017).

In general, WWTPs provide the initial opportunity for removing TOrCs and preventing significant environmental exposure. However, conventional wastewater treatment processes are not originally designed to eliminate diverging TOrCs (Grandclément *et al*. 2017). WWTPs are an important source for the entry of TOrCs; therefore, engineering solutions to improve the removal of TOrCs are needed. Recently, advanced physico-chemical treatment options such as ozonation and activated carbon have been developed and applied at full scale (Kosek *et al*. 2020). In addition, membrane filtration options and advance oxidation processes are also able to efficiently remove TOrCs but are cost intensive (Kanaujiya *et al*. 2019). Conventional activated sludge (CAS) reduces the overall load of micropollutants by both sorption and biodegradation processes but many compounds are only partially removed or persistent (Fischer *et al*. 2014). It has been shown that some of these more persistent compounds are well degraded in subsequent biofiltration systems (Paredes *et al*. 2016; Devault *et al*. 2021). For instance, the removal efficiencies of diclofenac by activated sludge ranged

from 20-30% (Zhang *et al*. 2008), while in slow sand filtration systems the removal rate was 35-42% (Matamoros *et al*. 2009; Scheytt *et al*. 2006; Casas *et al*. 2015).

Microbial communities bear a high potential to eliminate TOrCs via enzymatic degradation processes, and many recent studies have focused on the influences of various operation parameters to optimize TOrCs removal performance. So far, especially redox conditions (Oberleitner *et al*. 2020), carbon and nitrogen availability (Moe *et al*. 2001; Zhang *et al*. 2019), hydraulic retention time (Priya *et al*. 2015), and the filter material (Paredes *et al*. 2016) have been reported to affect the efficiency of different biofiltration systems. These studies have contributed to our understanding of micropollutant biotransformation in engineered systems. However, all of the aforementioned operating conditions have not a direct impact but rather affect the microbial communities and thereby the diversity and abundance and function of microorganisms.

To date, the micropollutant biotransformation mechanisms as well as the underlying drivers behind the degradation processes remains elusive. Therefore, to uncover the microbial "black box", more researches regarding the associations between the abundance of taxa, enzymes, pathways and TOrCs biotransformation are required. Johnson *et al*. (2015) for example investigated the taxonomic biodiversity and biotransformation rates of ten micropollutants in ten full-scale WWTPs, and found biodiversity was positively associated with the collective removal rates of TOrCs. To explore the biodiversity in more detail, Wolff *et al*. (2018) divided the general microbial community into a core and a specialized community and compared their composition with micropollutant removal in five different biological wastewater treatment systems. The results demonstrated the significant correlation between the relative abundance of specialized community members and the removal rates of certain compounds. For example, the abundances of the genera *Luteimonas*, *Roseibaca* and *Phenylobacterium* might be indicative for the degradation of metoprolol, 10,11-dihydro-10-hydrocarbamazepine and diclofenac under aerobic condition. Functional enzymes and degradation pathways are often studied in pure culture or individual compound biodegradation studies (Kjeldal *et al*. 2019), as the enzymatic reactions involving diverse microorganisms are quite intricate, making it hard to interpret the degradation pathways (Achermann *et al*. 2018; Zumstein *et al*. 2019). Despite these initial studies, the biotransformation mechanisms of various TOrCs in the biological filtration system on the microbial community level are rarely addressed so far, only few studies focused on their removal efficiencies and influencing factors (Zearley *et al*. 2012; Rattier *et al*. 2014; Carpenter *et al*. 2017).

In this study, biotransformation performance of eight different biological active sand filter materials from wastewater and water treatment plants for transforming 51 polar TOrCs were investigated experimentally. We coupled biotransformation rates with multiple microbial parameters, which involved the detailed analysis of degrading microorganisms, their encoded enzymes and transformation pathways. The aim of this study is: (1) to assess and compare the transformation efficiencies of different types of biological active systems in a fully controlled laboratory setup, (2) to evaluate the influence of the microbial community composition on the biotransformations, (3) to suggest novel biological indicators for a more comprehensive evaluation of individual or global TOrCs removal efficiencies. For this purpose, we put the eight sand filters under strictly controlled laboratory conditions, thereby excluding any influence of the above-mentioned parameters (redox conditions, carbon and nitrogen availability, hydraulic retention time) on differences in biotransformation rates. Hence, we focused on the transformation potential of the microbial communities at identical conditions, which allowed us to directly link biotransformation rates with taxa, genes and biomass markers. We hypothesize that differences in biotransformation rates will be mirrored by the a) microbial community, and their b) enzymatic repertoire encoded in the metagenome. Moreover, we evaluated which role biomass plays in the normalization of global transformation performance. This may lead to the identification of biological parameters for the removal of TOrCs, individually or globally.

Materials and methods

Trace organic compounds

51 polar TOrCs which have been typically found in municipal wastewater were selected as target compounds in this study (Table 1), including pesticides, pharmaceuticals, and personal care products with different biodegradabilities in CAS treatment. For example, acyclovir, atenolol, caffeine, and ibuprofen can be relatively easily degraded (Prasse *et al*. 2011; Ferrando-Climent *et al*. 2012; Xu *et al*. 2017a; Chtourou *et al*. 2018), while carbamazepine and diclofenac are persistent and difficult to be biotransformed (Kruglova *et al*. 2014; Zhang *et al*. 2008), and some compounds such as emtricitabine and cetirizin have only been rarely studied so far.

Experimental setup and operation

Six different sand materials from rapid sand filters of municipal WWTPs and two materials from slow sand filters used for water treatment were sampled and then stored at 4 °C for approximately three months. The batch experiments were performed in triplicates with all eight sand filters under the same conditions: 20 g of sand material was added to each 250 mL bottle and 80 mL of treated wastewater from the WWTP Koblenz. All batches were aerated with 7 $mg \cdot L^{-1}$ oxygen and

continuously shaken at 22 °C and the speed of 100 rpm in the dark. To acclimate the microorganisms, all batches were equilibrated to the experimental conditions for approximately 24 h before the experiment started. The experiment was started by spiking the bottles with a mixture of 51 TOrCs at the initial concentration of 0.5 $\mu g \cdot L^{-1}$ for each compound, which was within the range of TOrCs concentration in actual wastewater (Luo *et al*. 2014).

Sampling

Over 72 h incubation, water samples were withdrawn from the batches at regular intervals resulting in eight time points (0, 1, 4, 8, 12, 24, 48, 72 h). Samples were immediately filtered using 0.45 µm regenerated cellulose membrane (Macherey-Nagel, Germany) and stored at 4 °C for maximum 2 weeks until liquid chromatography tandem mass spectrometry (LC-MS/MS) analysis. At the end of the experiment, the remaining water was removed and the sand materials were collected and stored at -80 °C for DNA extraction. In addition, each sand material was fixed 1:1 with ethanol for fluorescence *in situ* hybridization (FISH) analysis.

Biomass measurement and FISH analysis

Loss on ignition was determined by drying 15 g of sand filter material at 105 °C overnight, and then placing in a muffle furnace at 440 °C for 4 h, weighing the samples at each step. ATP from 1 g sand filter material was measured by the single tube luminometer Sirius FB12 (Titertek Berthold, Germany) using the ATP Biomass Kit HS (BioThema, Sweden) according to the manufacturer's instructions with eight measurement points prior and after ATP standard addition. The ethanol fixed samples were sent to Vermicon AG (Munich, Germany) for cell count measurement and FISH analysis. In detail, 10 g samples of aggregate were vortexed (3 min), then treated in an ultrasonic bath (5 min), followed by vortexing (3 min). The surrounding liquid was diluted 1:1 with ethanol and mixed. A set of fluorescently labeled gene probes was used to identify different phyla and classes of bacteria with a fluorescence microscope. The total cell counts (live and dead cells) were quantified with 4,6-Diamidino-2-phenylindol-dihydrochloride (DAPI) staining after filtration through a 0.2 µm pore-size filter membrane and determination of the relative amount of viable bacteria.

LC-MS/MS measurement and calculation of biotransformation rates

To determine the concentrations of the 51 spiked TOrCs, all filtered samples of the eight time points were used for LC-MS/MS analysis via an Agilent 1260-LC coupled to a SCIEX QTrap 5500-MS according to the method previously described by Falås *et al.* (2016). Biotransformation rate constants were estimated assuming first-order kinetics and negligible sorption according to equation

(1), whereby S is the TOrCs concentration ($\mu g \cdot L^{-1}$), $X_{Biomass}$ is the biomass concentration represented by the ATP ($pmol \cdot g^{-1}$), and k_{biol} is the normalized pseudo-first-order rate constant in $g \cdot (pmol \cdot d)^{-1}$.

$$\frac{dS}{dt} = -k_{biol} * X_{Biomass} * S \quad (1)$$

DNA extraction and sequencing

The DNA of the microorganisms was extracted from the sand filter material, and was used to analyze the present taxa by 16S rRNA amplicon sequencing, and by whole genome shotgun sequencing. Approximately 1.5 g of the frozen filter material from the end of the experiment (24 samples) was used for DNA extraction using the FastDNA SPIN Kit for soil (MP Biomedicals, Eschwege, Germany) according to the manufacturer's instructions. Concentrations and purity of the individual DNA extracts were measured by microspectrophotometry (NanoPhotometer P330, Implen). 16S rRNA gene amplification, library preparation and sequencing was performed by IMGM Laboratories GmbH (Planegg, Germany). In short, primer pair 341F (CCTACGGGNGGCWGCAG) and 805R (GACTACHVGGGTATCTAATCC) for V3-V4 hypervariable region was used for amplification of the 16S gene. Next, the purified PCR products were normalized to equimolar concentration with the SequalPrep Normalization Plate Kit (Thermo Fisher Scientific) and the DNA library was sequenced on the Illumina MiSeq next generation sequencing system (Illumina Inc.) in paired end mode with 2 x 250 bp. Whole metagenome sequencing was performed by IMGM Laboratories GmbH (Planegg, Germany). In brief, the extracted DNA samples were checked for quality and quantity by a 1% agarose gel (Midori Green-stained) electrophoresis and a Qubit dsDNA HS Assay Kit (Invitrogen). Prior to library preparation, the high molecular weight gDNA was sheared to target fragment size of 550 bp using a Covaris M220 Focused-ultrasonicator (Brighton, United Kingdom). In the following, DNA was prepared for sequencing using the NEBnext UltraTM II DNA library preparation kit for Illumina (New England Biolabs). Sequence data were generated on the Illumina HiSeq 2500 next generation sequencing system with the 2 x 250 bp paired end mode. 16S and whole metagenome sequence data were deposited at ENA under the accession number PRJEB43767.

Data processing

All 16S rRNA gene amplicons data were processed in R (v 3.6.0) (R Core Team 2016) using DADA2 (v 1.9.0) pipeline (Callahan *et al*. 2016). Quality trimming, denoising, error-correction, paired-end read merging, chimera removal, and dereplication steps were performed according to the default setting. The amplicon sequence variants (ASVs) were taxonomically classified with a naïve

Bayesian classifier using the SILVA training dataset (v137) (Quast *et al.* 2013). The ASV and taxonomy tables, along with associated sample metadata were imported into phyloseq (v 1.22.3) (McMurdie and Holmes 2013) for community analysis. Whole metagenome sequencing data was processed using Trimmomatic (v 0.39) (Bolger *et al.* 2014), and the quality of the reads was checked with FastQC (v 0.11.8) (Andrews 2010). The metagenome data was used for a) validating the amplicon results with METAXA2 software (v 2.1.1) (Bengtsson-Palme *et al.* 2015); b) calculating the metagenomic distances between the samples by making a gene-pool comparison/relatedness determination with the k-mer based weighted inner product, kWIP (Murray *et al.* 2017); c) metagenome assembly and functional analysis. For these latter two analysis, we used MEGAHIT (v 1.2.9) (Li *et al.* 2015) to assemble the data, and QUAST (v 5.0.2) (Gurevich *et al.* 2013) to evaluate the assembly quality. For the subsequent functional analysis, SUPER-FOCUS (v 0.31) (Silva *et al.* 2015) was applied using the aligner DIAMOND (v 0.9.34) (Buchfink *et al.* 2015). In addition, taxonomic informed pathways classifications by sample groups were determined by HUMAnN2 (v 2.8.1) (Franzosa *et al.* 2018). Metagenome-assembled genomes (MAGs) were obtained by MetaBAT2 (v 2.15) (Kang *et al.* 2019) and manually refined after assessing the completeness (> 70%) and contamination (< 10%) by CheckM (v 1.0.13) (Parks *et al.* 2015). Taxonomic classification was conducted by GTDB-Tk (Chaumeil *et al.* 2020). Prodigal (v 2.6.3) (Hyatt *et al.* 2010) was used for open reading frames (ORFs) prediction. KofamKOALA (https://www.genome.jp/tools/kofamkoala/) (Aramaki *et al.* 2020) was used to obtain KO annotations for genes predicted by Prodigal. Xenobiotics metabolism was performed by the "Reconstruct Pathway" tool in KEGG mapper (https://www.genome.jp/kegg/mapper.html, accessed February 2021).

Statistical analysis

All statistical analysis were performed in R environment (v 3.6.0). *cor.test* function was used to test the correlation coefficient *r* between the TOrCs biotransformation performance and different biomass indicators based on the Pearson method. Linear model was used to describe the relationship between the global compound removal, k_{biol}, and ATP concentration. Residuals were tested for normality (Shapiro-Wilk normality test), and the distribution was inspected through QQ (quantile-quantile) plot (Figure S5). A paired two-sample Mann-Whitney-Wilcoxon test (non-parametric) was used to identify significant differences between k_{biol} values of two sand groups. Kruskal-Wallis test was used to evaluate the differences of individual compound k_{biol} among all sand samples and between categories. The relationships between DADA2 and METAXA2 data were examined by Mantel tests. The microbial diversity indices were analyzed using the vegan package (v 2.5-6) (Oksanen *et al.* 2019). The species richness was determined by rarefying the amplicon

dataset to the smallest sample (5799 reads) through the "rrarefy" function. Chao1 and Inverse Simpson index were used to present community richness and alpha diversity, respectively. Community compositions were compared using Bray-Curtis dissimilarities on ASV abundances and presented using NMDS ordinations. Ordinations and heatmaps were done in the R package "ampvis2" (v 2.4.6) (Andersen *et al.* 2018). The analysis of correlations between TOrCs biotransformation rates and microorganisms or enzymatic encoding genes was based on Pearson correlations outlined in the Rhea script collection (Lagkouvardos *et al.* 2017). Before doing the correlation analysis, we tested the differences between each compound k_{biol} and zero (criterion 1), and set the minimum removal percentage to 10% (criterion 2). As a consequence, the k_{biol} of carbamazipine, fluconazole and xipamide were excluded from further analysis, since either criterion 1 or 2 was not met in any of the batches. Differential enzymes and pathway analyses were conducted by DESeq2 (v 1.29.5) (Love *et al.* 2014).

Results

TOrCs biotransformation performance

Physical, chemical and biological characteristics of eight sand filters are shown in Table 2. Materials of these filter included quartz gravel, quartz sand, anthracite and pumice. Loss on ignition, ATP, DNA concentration and cell counts served as biomass indicators. Biomass was high in Friedrichshafen, Eriskirchen and Wangen (> 25 pmol/g ATP, > 40 mg/g Loss on ignition), while the remaining five biofilters were low in biomass, with lowest measurements in the filter materials from drinking water systems (BWA and IFW; < 1.5 pmol/g ATP, < 9 mg/g Loss on ignition) (Table 2, Fig. 1b). The biotransformation rate constants of TOrCs were calculated excluding six compounds (i.e., acridone, caffeine, ibuprofen, levetiracetam acid, ramiprilat and valsartan) which did not fit the first-order kinetics. Moreover, carbamazepine, fluconazol, xipamide had non-significant k_{biol} and showed less than 10% removal in all sand samples. Wangen achieved the best overall TOrC parent compound removal with a global mean removal percentage of 58%, followed by Friedrichshafen (49%) and Eriskirchen (45%) (Fig. 1a). Hungen and Stuttgart showed similar global removal percentages of 28% and 26%, followed by Moos with 14%, respectively. In the drinking water filters IFW and BWA, there were almost no TOrCs degraded (removal below 0.5%). These differences in global transformation potential were highly correlated with biomass expressed as ATP concentration (Pearson r = 0.92, p < 0.001), followed by living cell counts (Pearson r = 0.76, p < 0.001), while loss on ignition, which has been traditionally used for the k_{biol} normalization showed no correlation (Table 2). The mean global k_{biol} could be predicted by ATP concentration (ln(ATP); LM, t = 8.3, adjusted R^2 = 0.76, p < 0.001, Fig. 1c). Moreover, the overall average removal percentage showed a clear relationship with ATP concentration, also on a natural

logarithmic scale (LM, t = 13.9, adjusted R^2 = 0.90, p < 0.001, Fig. 1d). Therefore, we used ATP for $X_{Biomass}$ normalization (equation 1) of k_{biol} for the clustering analysis and the following correlation analysis. According to the ATP biomass, the samples with high biomass (Eriskirchen, Friedrichshafen and Wangen, named as HBG) had a high general biotransformation ability, while the biotransformation potential of the samples with low biomass (Hungen, Moos and Stuttgart, named as LBG) was relatively low, which can be also seen across individual compounds with exceptions (Fig. 2a). After ATP normalization, however, the individual differences between filter materials and compounds became less pronounced (Fig. 2b, except IFW). When comparing DW with the other two groups, their k_{biol} (mean value of individual substances in each group) were still different (Mann-Whitney-Wilcoxon test, W = 1305, p = 0.02 for HBG; W = 1318, p = 0.01 for LBG). However, when testing for differences in biotransformation of LBG and HBG, there was no significant difference in the mean global k_{biol} between the two groups (Mann-Whitney-Wilcoxon test, W = 1305, p = 0.33), indicating their mean biotransformation performance were comparable per biomass unit, independent of other parameters such as microbial community composition. On the other hand, differences between the k_{biol} of individual compounds persisted when comparing seven sand samples (IFW was excluded: the values close or below zero caused superimposed signals when normalized, Fig. 2b) or HBG and LBG. Overall, 19 compounds showed significant differences in seven sand samples, and 15 substances showed significantly differential k_{biol} between HBG and LBG (Kruskal-Wallis test, adjusted p < 0.05) (Table 1). For comparison, we found 35 and 38 substances to differ in their k_{biol} before normalization for the sand filter materials and HBG vs. LBG, respectively.

Taxonomic composition

To shed light on the microbial perspective of the filter materials, we investigated the microbial community composition of all incubations using 16S rRNA sequencing. All sequences were clustered into a total of 23147 bacterial ASVs after filtering step, showing obvious differences among the sand filters at the phylum level (Fig 3a). Apart from Proteobacteria that dominated in all filter materials, Nitrospirae dominated in the HBG with mean read abundances of 27.6%, followed by Bacteroidetes (11.5%). In the LBG, Nitrospirae only accounted for 0.7%. Microbial community composition was also analyzed using FISH, and METAXA2 based on metagenome derived ribosomal sequences (Fig. 3a), confirming the larger changes in relative abundances that we saw at the phylum level in the amplicon data. In particular, METAXA2 and DADA2 data were highly correlated in their community composition (Mantel tests, r = 0.96, p = 0.001). The FISH results confirmed that the relative proportion of cells and their respective biomass (assuming the same cell

size) follow the results of the DNA based data (with exceptions; e.g., for the Nitrospirae community in Stuttgart).

At the genus level, a high degree of variation in the taxonomic composition between the sand samples was observed (Fig. 3b, Fig S2). In the HBG, there was a high amount of *Nitrospira* in Wangen and Eriskirchen with mean relative abundances of 45.2% and 39.0%, respectively. In Friedrichshafen (which was operated for post-denitrification), *Nitrospira* only accounted for 3.6% and other lineages became more abundant (e.g., *Propionivibrio*, *Geobacter*, *Romboutsia*, *Legionella*). In LBG, the three sand samples exhibited largely different microbial composition without sharing abundant genera. *Stenotrophobacter* (24.4%) was prominent in Hungen and *Dokdonella* (17.8%) dominated the Stuttgart filter materials. *Pseudomonas* (20.1%) and *Janthinobacterium* (17.3%) were dominant in Moos. In contrast to HBG and LBG, DW showed a stark dominance of *Pseudomonas* with a mean relative abundance of 60.1%, which also resulted in the lowest biodiversity indices (Table 2). In a multivariate analysis of the community composition (presented as ASV or as k-mers derived from the metagenome) we could recover a separation into HBG and LBG (Fig. S3, adonis: for ASV, $R^2 = 0.21$, $p = 0.001$; for k-mers, $R^2 = 0.19$, $p = 0.001$).

Correlation of TOrCs biotransformation with microorganisms and functional enzymes

We observed a global correlation between the taxonomic composition (DADA2 and METAXA2) and the (normalized) k_{biol} (Mantel tests, $r = 0.50$, $p = 0.001$, for both matrices). Subsequently, Pearson's coefficients r were used to find hypothetical linkages between the k_{biol} and relative abundances of a) microbial genera (Fig. 4a); b) functional enzymes (Fig. 4b, see paragraph below). There were 62 genera that showed either a significantly positive or negative correlation with the biotransformation rates of TOrCs (with a cutoff of abs(r) > 0.7, adjusted $p < 0.05$, observation > 9) (Fig. 4a). 30 genera showed highly positive correlation with more than one TOrC, such as *Denitratisoma*, *Hydrogenophaga* and *Ideonella*; 4 genera only correlated with single TOrCs, e.g., *Litorilinea*, *Novosphingobium*, *Paludibaculum*, *Phaeodactylibacter* were only positively associated with the biotransformation of diclofenac, acyclovir, sulfamethoxazole and bezafibrate, respectively. To our surprise, *Nitrospira,* the dominant genus in the HBG, had no significant correlation with any compound. Examples for the negative correlation were *Conexibacter*, *Ferruginibacter*, *Intestinibacter*, *Methylibium*, *Pseudomonas* and *Terrimonas*. All these correlating microorganisms (except *Pseudomonas*) were ranked below 2% relative abundance and can be regarded as rare taxa.

When we look at the metagenome sequences, we could annotate 20409 enzymes. Principle component analysis (PCA) based on the relative abundance of annotated functional enzymes

demonstrated, similar to the taxonomic patterns described above, distinct clustering of different sand samples (Fig. 5). We can observe a separation between the HBG and LBG on the axis 2 (PC2, 12%) with the exception of Friedrichshafen that shifted towards LBG, maybe caused by the low abundance of *Nitrospira*. From LBG, Moos shifted on axis 1 (PC1, 78%) towards the distal DW. When comparing HBG with LBG, we detected that 1017 enzymes were over-represented in HBG and 1702 ones were over-represented in LBG, respectively (Fig. S1). We selected those responsible for biocatalysis/biodegradation according to EAWAG-BBD database and analyzed their associations with TOrCs biotransformation. As a result, there were in total 30 of 2079 functional enzymes that showed a correlation with TOrCs biotransformation (with a cutoff of abs(r) > 0.7, adjusted $p < 0.05$, observation > 9) (Fig. 4b). Notably, enoyl-CoA hydratase (EC 4.2.1.17)/3-hydroxyacyl-CoA dehydrogenase (EC 1.1.1.35) was positively correlated with eight compounds (i.e., benzotriazole, carboxy acyclovir, ceterizin, DEET, lamotrigine, mecoprop, terbuthylazine, torasemid). Both, dissimilatory sulfite reductase (EC 1.8.99.3) and nitrite reductase (EC 1.7.2.1), which are universal and essential enzymes in the sulfur and nitrogen cycle, were also correlated to the biotransformation of carboxy acyclovir, clarithromycin, furosemide and mecoprop. Further, a few enzymes showed a correlation to only a single compound removal rate. For example, amidase (EC 3.5.1.4) was found to be only correlated to the k_{biol} of carboxy acyclovir; threonine dehydratase (EC 4.3.1.19); acyl-CoA dehydrogenase, benzoate degradation ring-cleavage hydrolase, nitrate reductase (EC 1.7.2.1), S-formylglutathione hydrolase (EC 3.1.2.12) were only correlated with the removal rate of atenolol.

Biotransformation pathways analysis

Overall, there were 163 significantly differential pathways annotated by HUMAnN2 comparing the HBG with LBG. These pathways were demonstrated in Fig. S4 excluding biosynthesis pathways. In the HBG, sulfate reduction, aromatic biogenic amine degradation and pathways regarding carbohydrate degradation (i.e. starch, glycogen, stachyose, D−galactose, galactose degradation) were abundant, the involved microorganisms were identified to be mainly Nitrospirae. In the LBG, energy metabolism pathway, such as TCA cycle, Calvin-Benson-Bassham cycle, NAD/NADP−NADH/NADPH cytosolic interconversion were more pronounced, octane oxidation was also prominently abundant. To further explore biotransformation pathways based on the metagenome data, we had a closer look at MAGs for which we found correlations with individual k_{biol} (Fig. 4a, genera with green bars). These were put into the KEGG Mapper for pathway reconstruction and we estimated the completeness of the pathways for each MAG (Fig. 6). In the category of xenobiotics metabolism, MAGs classified to *Hydrogenophaga* showed the most complete pathways, especially in benzoate and furfural degradation. Steroid degradation pathway was prominent in *Sphingorhabdus* and *Pseudomonas*.

Discussion

Currently, parameters such as redox conditions or biodegradable dissolved organic carbon, are used to evaluate the removal efficiencies of TOrCs (Bertelkamp *et al*. 2016; Torresi *et al*. 2019; Oberleitner *et al*. 2020), but new indicators directly associated to degradation processes (e.g., microorganisms, functional enzymes, transformation products) can be expected to be additional suitable tools for the prediction of the biotransformation potential and controlling removal performance. Here, we investigated the biotransformation of diverging TOrCs by eight biological active sand filter materials from wastewater and drinking water treatment plants, for which the metagenomic analysis of the microbial communities provided novel insights into the biological potential of TOrC transformations.

Microbial biomass indicators and the potential role of rare taxa for biotransformations

In general, we divided the filters into three groups according to the clustering results, microbial community composition, and their biomass estimates. The taxonomic composition between the HBG, LBG, DW, and also between single sand filters was very different. HBG, though, shared Nitrospirae as highly abundant lineage (Fig. 3), a diverse and widespread group of often autotrophic, nitrite-oxidizing bacteria (Koch *et al*. 2015). Previous studies found that biotransformation of certain TOrCs can be related to ammonia oxidation activity of nitrifying activated sludge and biofilms in WWTPs (Helbling *et al*. 2012; Rattier *et al*. 2014; Men *et al*. 2017; Xu *et al*. 2017b). Moreover, asulam, carbendazim, fenhexamid, mianserin, and ranitidine showed biotransformation (16-85%) by the isolate *Nitrospira inopinata* (Han *et al*. 2019). Metagenome data of rapid gravity sand filter microorganisms also suggested that *Nitrospira* may serve as keystone species that drives the microbial ecosystems by providing organic carbon compounds and enable heterotrophic ammonium and carbon cycling (Palomo *et al*. 2016). In our system, we found no direct statistical linkage between *Nitrospira* and the biotransformation rate constants, however, it is possible that at least in the investigated biofilters Nitrospirae lineages as autotrophic species enables the establishment of a high microbial biomass, and thus enables the TOrC transformations through other microbial members. This also matches the observations by Liang *et al*. (2021), which indicates that the biotransformation may rely on rare community members of TOrCs-specific degraders, while the community of their moving bed reactor followed a progressive succession towards a Nitrospirae based climax community. The hypothesized positive and negative linkages of TOrC biotransformation with microbial genera pointed to rare biosphere microorganisms (< 2%), which exhibited most of the correlations with individual TOrCs removal rates. Although our correlations are only statistical based result, and still need experimental verification to test a causal

relationship, these correlation-based hypothesis are in line with previous reports indicating that a small fraction of highly-specialized microorganisms, accounting for less than 0.1% of the microbial communities in biofilms may be responsible for the TOrC transformation (Falås *et al*. 2018). One of the highly correlating genera was *Hydrogenophaga*, which showed a putative linkage to the removal of amisulprid, clarithromycin, climbazole, flecainide, oxypurinol, sitagliptine, sulpirid, terbutryn and venlafaxine (the top left cluster in Fig. 4a). This genus has also been previously reported to efficiently remove diclofenac, metoprolol, clarithromycin, erythromycin, atenolol and codeine (Kanaujiya *et al*. 2019).

In the drinking water sand filters DW, the biotransformation performance significantly differed from the wastewater filters. Here, *Pseudomonas* was found dominating DW, a common inhabitant of aquatic environments, including oligotrophic drinking water, lake water and surface water (Lopez *et al*. 2005; Huang *et al*. 2015; Nasreen *et al*. 2015). Although it has been reported to be able to degrade certain micropollutants (Li *et al*. 2010; Tezel *et al*. 2012; Devi *et al*. 2019), in our case, it also clustered in proximity to *Hydrogenophaga*, however, with more pronounced negative correlations with TOrCs.

Taxa and enzymatic correlations with biotransformation rates

The abundance of functional enzymes and biotransformation pathways also correlated with individual compounds and resulted in a clearer clustering than the microbial lineages. Enoyl-CoA hydratase/3-hydroxyacyl-CoA dehydrogenase was overrepresented in the HBG and was positively correlated with eight TOrCs in our study. The enoyl-CoA hydratase is known to catalyze a β-oxidation substrate by adding hydroxyl groups and a proton to an unsaturated β-carbon of the molecule (Salgado *et al*. 2020). For instance, the degradation of ibuprofen can be initiated by enoyl-CoA hydratase with the introduction of hydroxyl groups, this enzyme was found to be up-regulated during the biodegradation process (Kjeldal *et al*. 2012). Enoyl-CoA hydratase was also identified in steroid estrogen degradation by bacterium *Serratia nematodiphila* (Zhao *et al*. 2020). Furthermore, Carmeron *et al*. (2019) reported enoyl-CoA hydratase contributed to biofilm formation and the antibiotic tolerance, which also supported our findings that the high biomass promoted the TOrCs removal. Therefore, we suggest that a high abundance of enoyl-CoA hydratase/3-hydroxyacyl-CoA dehydrogenase genes might indicate a favorable functional potential for TOrCs biotransformation. Dissimilatory sulfite reductase (EC 1.8.99.3) and nitrite reductase (EC 1.7.2.1) were found to be correlated to the biotransformation of carboxy acyclovir, clarithromycin, furosemide and mecoprop in our study. In previous researches, sulfite reductase was reported to catalyze the cleavage of isoxazole and piperazinyl rings (Jia *et al*. 2019), and nitrite reductase was correlated with the

biotransformation rate constant of some compounds like sulfamethoxazole, erythromycin and trimethoprim (Torresi *et al.* 2018). However, more studies are needed to further support this association and to investigate whether this can be explained by any causal relationship.

ATP as new predictor for biotransformation potential and normalization

One of the most surprising results was that despite these largely differing taxonomic and enzymatic profiles of each sand filter, the strong differences in the overall biotransformation performance (-1.4% vs 58% removal) across all investigated TOrCs were mostly eliminated after accounting for biomass, measured as ATP. This indicates that we can predict the global transformation potential of (*ex situ*) materials from biofilters largely (explaining 76% of the k_{biol} variation or 90% of the variation for compound removal) by measuring the living biomass as ATP concentration. Biomass has been introduced as a parameter for TOrCs biotransformation kinetics. The biotransformation rate constants k_{biol} are usually normalized by attached or suspended biomass as e.g. dry weight (Mazioti *et al*. 2015; Torresi *et al*. 2016), total suspended solids (Achermann *et al*. 2018), or DNA concentration (Liang *et al*. 2021). However, very few studies investigated the biotransformation differences under the normalized and non-normalized condition (Casas *et al*. 2015), and to the best of our knowledge there is no report on the correlation analysis of various biomass indicators with biotransformation rates. Our findings suggest that at least for biofiltration systems the global potential for the biotransformation of TOrCs is more dependent on ATP than on other biomass indicators. Hence, ATP could have a profound impact on the biotransformation of TOrCs and their research. Previous studies could have been at least partially biased by dead cells (DNA measurements, and cell counts), EPS, and other adsorbed carbon compounds (total carbon based measurements, weight measurements, DNA). In our study, living and total cells (biased mainly by the different cell volumes) were still the best predictors after ATP (Table 2). Originally, the k_{biol} should be determined by the absolute abundance of the functional degraders of the respective TOrC (Bekins *et al*. 1998), however, in our scenario, the biomass does not really reflect the proportion of degraders (unless this proportion is constant within all communities). Other studies already found indications that biomass is important for overall system performance, e.g. Liang *et al.* (2021) observed that the biomass increased with the running time of the reactors when also the TOrC removal increased, and Torresi *et al*. (2016) observed an enhanced TOrC removal with an increased biofilm thickness, although this feature was simultaneously attributed to increased diversity. In our study, alpha-diversity showed no such correlation (Table 2). In contrast, our results imply that the effect of biomass as ATP on the global TOrC transformation potential is foremost independent of the microbial community composition. We therefore had to partially reject our hypothesis that the microbial community composition is the major driver between global biotransformation potential in

our experimental setup. However, on the other hand, the clear correlation of the compound matrix with the taxonomic matrix found by the Mantel test and later with single genera after normalization is evidence that although the global transformation potential is determined by biomass as ATP, the removal of individual compounds is related to the taxonomic composition of the biological active sand filter system. After normalization, we could still identify significant differences for more than 15 different compounds (Table 1, e.g. clarithromycin, mecoprop, metoprolol, trimethoprim, furosemide, atenolol), which may be good candidates for a rather taxa or community specific degradation.

Limitations and perspectives

Our study was designed to compare the biological transformation potential of the filter materials *ex situ* under controlled conditions by applying laboratory scale transformation batch experiments. However, factors such as engineering design, redox potential, water retention times, feed/famine cycles that can influence the bioactivity, were explicitly not considered here. Moreover, we mainly focused on filter systems used for post-treatment of conventionally treated wastewater, and thus our results may be more representative for these types of rapid sand filters that have already experienced long-term exposure to TOrCs. The selection of 51 polar compounds maybe not fully representative of the full spectrum of TOrCs, but they cover a typical range of biodegradable and persistent compounds that can be found in wastewater (Ahmad *et al*. 2019), and the historical exposure of sand filters avoids artifacts due to falsely adapted or artificial assembled microbial communities. Since the selected TOrCs are relatively polar compounds and for many of them organic carbon normalized distribution coefficients have been reported to be rather low (Ternes *et al*. 2004; Stein *et al.* 2008; Ramil *et al.* 2010), sorption was considered negligible and we assumed that the observed removal was mainly attributed to transformation processes. Future studies should test, whether ATP can also account for differences in *in situ* full-scale filters under natural retention times, if autotrophic taxa, such as Nitrospirae, can be indeed act as primary carbon and energy source that facilitates other taxa such as *Hydrogenophaga* for individual TOrC transformations. Finally, our findings can be used as hypothesis for further looking into the details of TOrC biotransformation and its relationship with single taxa or whole communities.

Conclusions

To summarize, we investigated the biotransformation performance of 51 TOrCs in eight sand filters from wastewater and drinking water treatment plants, and established associations between the microorganisms, functional enzymes and the TOrCs biotransformation. We conclude that

1. the global biotransformation potential can be predicted by measuring the total biomass as ATP. After normalization to ATP, there was no significant difference of the average k_{biol} between the main sand filter systems. This suggests that ATP is a main performance estimator;
2. the removal of individual compounds, however, is related to the taxonomic composition of the biological active sand filter system, indicated by individual k_{biol} correlation with single genera, and by the global correlation of the microbial community compositon with the normalized k_{biol} matrix;
3. biotransformations of several TOrCs were rather correlated to rare biosphere lineages, e.g., *Hydrogenophaga* that had the most complete xenobiotics degradation pathways; on the enzymatic level, Enoyl-CoA hydratase/3-hydroxyacyl-CoA dehydrogenase, showed the broadest correlation with individual TOrC k_{biol}.
4. both, certain species as well as enzymes, can serve as indicators for the degradation potential of microbial communities in biofiltration systems, which is also of high practical relevance as it could support the optimization and control of these systems.

Data availability statement

All sequence data has been deposited at INSDC (with ENA: https://www.ebi.ac.uk/ena) under the accession number PRJEB43767. The ASV table, MAGs, and the DESeq2 output can be inspected in the supplementary material.

Acknowledgment

Arne Wick and David Wolff would like to acknowledge the financial support of the research, which was part of the project OPTI (02WIL1388) funded by the German Federal Ministry of Education and Research (BMBF). Lijia Cao would like to acknowledge the financial support for her PhD study from the Chinese Scholarship Council. Renato Liguori would like to acknowledge the International PhD Programme “Environment, Resources and Sustainable Development” scholarship (#Parthenope University of Naples). Christian Wurzbacher would like to acknowledge the DFG grant for individual funding (WU 890/2-1), and we would like to thank the Leibniz-Rechenzentrum for providing computational support and Dr. Uwe Hübner for proof reading and a critical review of the manuscript. Dr. Claudia Beimfohr of Vermicon AG, Germany, is thanked for carrying out FISH analyses and cell count measurement.

Authors contributions

AW and DW designed and performed the experiment and the chemical analysis. LC, RL, and CW, analyzed the molecular data and made the statistical analysis. LC performed the metagenome

assembly. CW and LC developed and wrote the initial draft of the manuscript and all authors improved the manuscript sequentially by several rounds of review.

Reference

Achermann, S., Bianco, V., Mansfeldt, C. B., Vogler, B., Kolvenbach, B. A., Corvini, P. F., & Fenner, K. (2018). Biotransformation of sulfonamide antibiotics in activated sludge: the formation of pterin-conjugates leads to sustained risk. Environmental science & technology, 52(11), 6265-6274.

Ahmad, J., Naeem, S., Ahmad, M., Usman, A. R., & Al-Wabel, M. I. (2019). A critical review on organic micropollutants contamination in wastewater and removal through carbon nanotubes. Journal of environmental management, 246, 214-228.

Andersen, K. S., Kirkegaard, R. H., Karst, S. M., & Albertsen, M. (2018). ampvis2: an R package to analyse and visualise 16S rRNA amplicon data. BioRxiv, 299537.

Andrews, S. (2010). FastQC: A quality control tool for high throughput sequence data [Online]. Available online at: http://www.bioinformatics.babraham.ac.uk/projects/fastqc/

Aramaki, T., Blanc-Mathieu, R., Endo, H., Ohkubo, K., Kanehisa, M., Goto, S., & Ogata, H. (2020). KofamKOALA: KEGG ortholog assignment based on profile HMM and adaptive score threshold. Bioinformatics, 36(7), 2251-2252.

Bekins, B. A., Warren, E., & Godsy, E. M. (1998). A comparison of zero order, first order, and monod biotransformation models. Groundwater, 36(2), 261-268.

Bengtsson Palme, J., Hartmann, M., Eriksson, K. M., Pal, C., Thorell, K., Larsson, D. G. J., & Nilsson, R. H. (2015). METAXA2: improved identification and taxonomic classification of small and large subunit rRNA in metagenomic data. Molecular ecology resources, 15(6), 1403-1414.

Bertelkamp, C., van der Hoek, J. P., Schoutteten, K., Hulpiau, L., Vanhaecke, L., Bussche, J. V., ... & Singhal, N. (2016). The effect of feed water dissolved organic carbon concentration and composition on organic micropollutant removal and microbial diversity in soil columns simulating river bank filtration. Chemosphere, 144, 932-939.

Bolger, A. M., Lohse, M., & Usadel, B. (2014). Trimmomatic: a flexible trimmer for Illumina sequence data. Bioinformatics, 30(15), 2114-2120.

Buchfink, B., Xie, C., & Huson, D. H. (2015). Fast and sensitive protein alignment using DIAMOND. Nature methods, 12(1), 59-60.

Callahan, B. J., McMurdie, P. J., Rosen, M. J., Han, A. W., Johnson, A. J. A., & Holmes, S. P. (2016). DADA2: high-resolution sample inference from Illumina amplicon data. Nature methods, 13(7), 581-583.

Cameron, L. C., Bonis, B., Phan, C. Q., Kent, L. A., Lee, A. K., & Hunter, R. C. (2019). A putative enoyl-CoA hydratase contributes to biofilm formation and the antibiotic tolerance of Achromobacter xylosoxidans. NPJ biofilms and microbiomes, 5(1), 1-7.

Carpenter, C. M., & Helbling, D. E. (2017). Removal of micropollutants in biofilters: Hydrodynamic effects on biofilm assembly and functioning. Water research, 120, 211-221.

Casas, M. E., Chhetri, R. K., Ooi, G., Hansen, K. M., Litty, K., Christensson, M., ... & Bester, K. (2015). Biodegradation of pharmaceuticals in hospital wastewater by staged Moving Bed Biofilm Reactors (MBBR). Water research, 83, 293-302.

Castronovo, S., Wick, A., Scheurer, M., Nödler, K., Schulz, M., & Ternes, T. A. (2017). Biodegradation of the artificial sweetener acesulfame in biological wastewater treatment and sandfilters. Water research, 110, 342-353.

Chaumeil, P. A., Mussig, A. J., Hugenholtz, P., & Parks, D. H. (2020). GTDB-Tk: a toolkit to classify genomes with the Genome Taxonomy Database. Bioinformatics, 36(6), 1925-1927.

Chtourou, M., Mallek, M., Dalmau, M., Mamo, J., Santos-Clotas, E., Salah, A. B., ... & Monclús, H. (2018). Triclosan, carbamazepine and caffeine removal by activated sludge system focusing on membrane bioreactor. Process Safety and Environmental Protection, 118, 1-9.

Devault, D. A., Amalric, L., Bristeau, S., Cruz, J., Tapie, N., Karolak, S., ... & Lévi, Y. (2021). Removal efficiency of emerging micropollutants in biofilter wastewater treatment plants in tropical areas. Environmental Science and Pollution Research, 28(9), 10940-10966.

Devi, R. S., Ramya, R., Kannan, K., Antony, A. R., & Kannan, V. R. (2019). Investigation of biodegradation potentials of high density polyethylene degrading marine bacteria isolated from the coastal regions of Tamil Nadu, India. Marine pollution bulletin, 138, 549-560.

Falås, P., Jewell, K. S., Hermes, N., Wick, A., Ternes, T. A., Joss, A., & Nielsen, J. L. (2018). Transformation, CO_2 formation and uptake of four organic micropollutants by carrier-attached microorganisms. Water research, 141, 405-416.

Falås, P., Wick, A., Castronovo, S., Habermacher, J., Ternes, T. A., & Joss, A. (2016). Tracing the limits of organic micropollutant removal in biological wastewater treatment. Water Research, 95, 240-249.

Ferrando-Climent, L., Collado, N., Buttiglieri, G., Gros, M., Rodriguez-Roda, I., Rodriguez-Mozaz, S., & Barceló, D. (2012). Comprehensive study of ibuprofen and its metabolites in activated sludge batch experiments and aquatic environment. Science of the Total Environment, 438, 404-413.

Fischer, K., & Majewsky, M. (2014). Cometabolic degradation of organic wastewater micropollutants by activated sludge and sludge-inherent microorganisms. Applied microbiology and biotechnology, 98(15), 6583-6597.

Franzosa, E. A., McIver, L. J., Rahnavard, G., Thompson, L. R., Schirmer, M., Weingart, G., ... & Huttenhower, C. (2018). Species-level functional profiling of metagenomes and metatranscriptomes. Nature methods, 15(11), 962-968.

Grandclément, C., Seyssiecq, I., Piram, A., Wong-Wah-Chung, P., Vanot, G., Tiliacos, N., ... & Doumenq, P. (2017). From the conventional biological wastewater treatment to hybrid processes, the evaluation of organic micropollutant removal: a review. Water research, 111, 297-317.

Gurevich, A., Saveliev, V., Vyahhi, N., & Tesler, G. (2013). QUAST: quality assessment tool for genome assemblies. Bioinformatics, 29(8), 1072-1075.

Han, P., Yu, Y., Zhou, L., Tian, Z., Li, Z., Hou, L., ... & Men, Y. (2019). Specific micropollutant biotransformation pattern by the comammox bacterium *Nitrospira inopinata*. Environmental science & technology, 53(15), 8695-8705.

Helbling, D. E., Johnson, D. R., Honti, M., & Fenner, K. (2012). Micropollutant biotransformation kinetics associate with WWTP process parameters and microbial community characteristics. Environmental science & technology, 46(19), 10579-10588.

Huang, T., Guo, L., Zhang, H., Su, J., Wen, G., & Zhang, K. (2015). Nitrogen-removal efficiency of a novel aerobic denitrifying bacterium, *Pseudomonas stutzeri* strain ZF31, isolated from a drinking-water reservoir. Bioresource technology, 196, 209-216.

Hyatt, D., Chen, GL., LoCascio, P.F. et al. (2010). Prodigal: prokaryotic gene recognition and translation initiation site identification. BMC Bioinformatics, 11(119).

Jia, Y., Zhang, H., Khanal, S. K., Yin, L., & Lu, H. (2019). Insights into pharmaceuticals removal in an anaerobic sulfate-reducing bacteria sludge system. Water research, 161, 191-201.

Johnson, D. R., Helbling, D. E., Lee, T. K., Park, J., Fenner, K., Kohler, H. P. E., & Ackermann, M. (2015). Association of biodiversity with the rates of micropollutant biotransformations among full-scale wastewater treatment plant communities. Applied and environmental microbiology, 81(2), 666-675.

Kanaujiya, D. K., Paul, T., Sinharoy, A., & Pakshirajan, K. (2019). Biological Treatment Processes for the Removal of Organic Micropollutants from Wastewater: a Review. Current pollution reports, 5(3), 112-128.

Kang, D. D., Li, F., Kirton, E., Thomas, A., Egan, R., An, H., & Wang, Z. (2019). MetaBAT 2: an adaptive binning algorithm for robust and efficient genome reconstruction from metagenome assemblies. PeerJ, 7, e7359.

Kjeldal, H., Lolas, I. B. Y., Knudsen, A. D., Carvalho, G., Nielsen, K. L., Crespo, M. T. B., ... &

Kundu, K., Marozava, S., Ehrl, B., Merl-Pham, J., Griebler, C., & Elsner, M. (2019). Defining lower limits of biodegradation: atrazine degradation regulated by mass transfer and maintenance demand in *Arthrobacter aurescens* TC1. The ISME journal, 13(9), 2236-2251.

Koch, H., Lücker, S., Albertsen, M., Kitzinger, K., Herbold, C., Spieck, E., ... & Daims, H. (2015). Expanded metabolic versatility of ubiquitous nitrite-oxidizing bacteria from the genus *Nitrospira*. Proceedings of the national academy of sciences, 112(36), 11371-11376.

Kosek, K., Luczkiewicz, A., Fudala-Książek, S., Jankowska, K., Szopińska, M., Svahn, O., ... & Björklund, E. (2020). Implementation of advanced micropollutants removal technologies in wastewater treatment plants (WWTPs)-Examples and challenges based on selected EU countries. Environmental science & policy, 112, 213-226.

Kruglova, A., Ahlgren, P., Korhonen, N., Rantanen, P., Mikola, A., & Vahala, R. (2014). Biodegradation of ibuprofen, diclofenac and carbamazepine in nitrifying activated sludge under 12 °C temperature conditions. Science of the total environment, 499, 394-401.

Lagkouvardos, I., Fischer, S., Kumar, N., & Clavel, T. (2017). Rhea: a transparent and modular R pipeline for microbial profiling based on 16S rRNA gene amplicons. PeerJ, 5, e2836.

Li, H., Li, X., Duan, Y., Zhang, K. Q., & Yang, J. (2010). Biotransformation of nicotine by microorganism: the case of *Pseudomonas* spp. Applied microbiology and biotechnology, 86(1), 11-17.

Li, D., Liu, C. M., Luo, R., Sadakane, K., & Lam, T. W. (2015). MEGAHIT: an ultra-fast single-node solution for large and complex metagenomics assembly via succinct de Bruijn graph. Bioinformatics, 31(10), 1674-1676.

Liang, C., de Jonge, N., Carvalho, P. N., Nielsen, J. L., & Bester, K. (2021). Biodegradation kinetics of organic micropollutants and microbial community dynamics in a moving bed biofilm reactor. Chemical engineering journal, 128963.

Lopez, L., Pozo, C., Rodelas, B., Calvo, C., Juarez, B., Martinez-Toledo, M. V., & Gonzalez-Lopez, J. (2005). Identification of bacteria isolated from an oligotrophic lake with pesticide removal capacities. Ecotoxicology, 14(3), 299-312.

Love, M. I., Huber, W., & Anders, S. (2014). Moderated estimation of fold change and dispersion for RNA-seq data with DESeq2. Genome biology, 15(12), 550.

Luo, Y., Guo, W., Ngo, H. H., Nghiem, L. D., Hai, F. I., Zhang, J., ... & Wang, X. C. (2014). A review on the occurrence of micropollutants in the aquatic environment and their fate and removal during wastewater treatment. Science of the total environment, 473, 619-641.

Matamoros, V., Arias, C., Brix, H., & Bayona, J. M. (2009). Preliminary screening of small-scale domestic wastewater treatment systems for removal of pharmaceutical and personal care products. Water research, 43(1), 55-62.

Mazioti, A. A., Stasinakis, A. S., Pantazi, Y., & Andersen, H. R. (2015). Biodegradation of benzotriazoles and hydroxy-benzothiazole in wastewater by activated sludge and moving bed biofilm reactor systems. Bioresource technology, 192, 627-635.

McMurdie, P. J., & Holmes, S. (2013). phyloseq: an R package for reproducible interactive analysis and graphics of microbiome census data. PloS one, 8(4), e61217.

Men, Y., Achermann, S., Helbling, D. E., Johnson, D. R., & Fenner, K. (2017). Relative contribution of ammonia oxidizing bacteria and other members of nitrifying activated sludge communities to micropollutant biotransformation. Water research, 109, 217-226.

Montiel-León, J. M., Duy, S. V., Munoz, G., Amyot, M., & Sauvé, S. (2018). Evaluation of on-line concentration coupled to liquid chromatography tandem mass spectrometry for the quantification of neonicotinoids and fipronil in surface water and tap water. Analytical and bioanalytical chemistry, 410(11), 2765-2779.

Moe, W. M., & Irvine, R. L. (2001). Effect of nitrogen limitation on performance of toluene degrading biofilters. Water Research, 35(6), 1407-1414.

Murray, K. D., Webers, C., Ong, C. S., Borevitz, J., & Warthmann, N. (2017). kWIP: The k-mer weighted inner product, a de novo estimator of genetic similarity. PLoS computational biology, 13(9), e1005727.

Naghdi, M., Taheran, M., Brar, S. K., Kermanshahi-pour, A., Verma, M., & Surampalli, R. Y. (2018). Biotransformation of carbamazepine by laccase-mediator system: Kinetics, by-products and toxicity assessment. Process Biochemistry, 67, 147-154.

Nasreen, M., Sarker, A., Malek, M. A., Ansaruzzaman, M. D., & Rahman, M. (2015). Prevalence and resistance pattern of Pseudomonas aeruginosa isolated from surface water. Advances in mcrobiology, 5(01), 74.

Oberleitner, D., Schulz, W., Bergmann, A., & Achten, C. (2020). Impact of seasonality, redox conditions, travel distances and initial concentrations on micropollutant removal during riverbank filtration at four sites. Chemosphere, 250, 126255.

Oksanen, J., Blanchet, F. G., Friendly, M., Kindt, R., Legendre, P., McGlinn, D., ... & Wagner, H. (2019). vegan: Community Ecology Package. R package version 2.5-6. 2019.

Palomo, A., Fowler, S. J., Gülay, A., Rasmussen, S., Sicheritz-Ponten, T., & Smets, B. F. (2016). Metagenomic analysis of rapid gravity sand filter microbial communities suggests novel physiology of *Nitrospira* spp. The ISME journal, 10(11), 2569-2581.

Parks D. H., Imelfort M., Skennerton C.T., Hugenholtz P., Tyson G.W. (2015). CheckM: assessing the quality of microbial genomes recoveredfrom isolates, single cells, and metagenomes. Genome research, 25, 1043–55.

Paredes, L., Fernandez-Fontaina, E., Lema, J. M., Omil, F., & Carballa, M. (2016). Understanding the fate of organic micropollutants in sand and granular activated carbon biofiltration systems. Science of the total environment, 551, 640-648.

Prasse, C., Wagner, M., Schulz, R., & Ternes, T. A. (2011). Biotransformation of the antiviral drugs acyclovir and penciclovir in activated sludge treatment. Environmental science & technology, 45(7), 2761-2769.

Priya, V. S., & Philip, L. (2015). Treatment of volatile organic compounds in pharmaceutical wastewater using submerged aerated biological filter. Chemical engineering journal, 266, 309-319.

Quast, C., Pruesse, E., Yilmaz, P., Gerken, J., Schweer, T., Yarza, P., Peplies, J., Glöckner, F. O. (2012). The SILVA ribosomal RNA gene database project: improved data processing and web-based tools. Nucleic acids research, 41(D1), D590-D596.

R Core Team. (2016). R: A Language and Environment for Statistical Computing. Vienna, Austria. Retrieved from https://www.R-project.org/

Ramil, M., El Aref, T., Fink, G., Scheurer, M., & Ternes, T. A. (2010). Fate of beta blockers in aquatic-sediment systems: sorption and biotransformation. Environmental science & technology, 44(3), 962-970.

Rattier, M., Reungoat, J., Keller, J., & Gernjak, W. (2014). Removal of micropollutants during tertiary wastewater treatment by biofiltration: role of nitrifiers and removal mechanisms. Water research, 54, 89-99.

Salgado, R., Brito, D., Noronha, J. P., Almeida, B., Bronze, M. R., Oehmen, A., ... & Barreto Crespo, M. T. (2020). Metabolite identification of ibuprofen biodegradation by *Patulibacter medicamentivorans* under aerobic conditions. Environmental technology, 41(4), 450-465.

Scheytt, T. J., Mersmann, P., & Heberer, T. (2006). Mobility of pharmaceuticals carbamazepine, diclofenac, ibuprofen, and propyphenazone in miscible-displacement experiments. Journal of contaminant hydrology, 83(1-2), 53-69.

Shao, Y., Chen, Z., Hollert, H., Zhou, S., Deutschmann, B., & Seiler, T. B. (2019). Toxicity of 10 organic micropollutants and their mixture: Implications for aquatic risk assessment. Science of the total environment, 666, 1273-1282.

Silva, G. G. Z., Green, K. T., Dutilh, B. E., & Edwards, R. A. (2016). SUPER-FOCUS: a tool for agile functional analysis of shotgun metagenomic data. Bioinformatics, 32(3), 354-361.

Stein, K., Ramil, M., Fink, G., Sander, M., & Ternes, T. A. (2008). Analysis and sorption of psychoactive drugs onto sediment. Environmental science & technology, 42(17), 6415-6423.

Tezel, U., Tandukar, M., Martinez, R. J., Sobecky, P. A., & Pavlostathis, S. G. (2012). Aerobic biotransformation of n-tetradecylbenzyldimethylammonium chloride by an enriched *Pseudomonas* spp. community. Environmental science & technology, 46(16), 8714-8722.

Torresi, E., Fowler, S. J., Polesel, F., Bester, K., Andersen, H. R., Smets, B. F., ... & Christensson, M. (2016). Biofilm thickness influences biodiversity in nitrifying MBBRs—Implications on micropollutant removal. Environmental science & technology, 50(17), 9279-9288.

Torresi, E., Gülay, A., Polesel, F., Jensen, M. M., Christensson, M., Smets, B. F., & Plósz, B. G. (2018). Reactor staging influences microbial community composition and diversity of denitrifying MBBRs-Implications on pharmaceutical removal. Water research, 138, 333-345.

Torresi, E., Tang, K., Deng, J., Sund, C., Smets, B. F., Christensson, M., & Andersen, H. R. (2019). Removal of micropollutants during biological phosphorus removal: Impact of redox conditions in MBBR. Science of the total environment, 663, 496-506.

Tröger, R., Klöckner, P., Ahrens, L., & Wiberg, K. (2018). Micropollutants in drinking water from source to tap-Method development and application of a multiresidue screening method. Science of the total environment, 627, 1404-1432.

Vieno, N., & Sillanpää, M. (2014). Fate of diclofenac in municipal wastewater treatment plant—a review. Environment international, 69, 28-39.

Wolff, D., Krah, D., Dötsch, A., Ghattas, A. K., Wick, A., & Ternes, T. A. (2018). Insights into the variability of microbial community composition and micropollutant degradation in diverse biological wastewater treatment systems. Water research, 143, 313-324.

Xu, Y., Yuan, Z., & Ni, B. J. (2017a). Biotransformation of acyclovir by an enriched nitrifying culture. Chemosphere, 170, 25-32.

Xu, Y., Yuan, Z., & Ni, B. J. (2017b). Impact of ammonium availability on atenolol biotransformation during nitrification. ACS Sustainable chemistry & engineering, 5(8), 7137-7144.

Yang, Y. Y., Toor, G. S., Wilson, P. C., & Williams, C. F. (2017). Micropollutants in groundwater from septic systems: Transformations, transport mechanisms, and human health risk assessment. Water research, 123, 258-267.

Zearley, T. L., & Summers, R. S. (2012). Removal of trace organic micropollutants by drinking water biological filters. Environmental science & technology, 46(17), 9412-9419.

Zhang, Y., Geißen, S. U., & Gal, C. (2008). Carbamazepine and diclofenac: removal in wastewater treatment plants and occurrence in water bodies. Chemosphere, 73(8), 1151-1161.

Zhang, L., Carvalho, P. N., Bollmann, U. E., Brix, H., & Bester, K. (2019). Enhanced removal of pharmaceuticals in a biofilter: Effects of manipulating co-degradation by carbon feeding. Chemosphere, 236, 124303.

Zhao, X., Wang, Y., Xu, X., Tian, K., Zhou, D., Meng, F., ... & Huo, H. (2020). Genomics analysis of the steroid estrogen-degrading bacterium *Serratia nematodiphila* DH-S01. Biotechnology & biotechnological equipment, 34(1), 430-440.

Zumstein, M. T., & Helbling, D. E. (2019). Biotransformation of antibiotics: exploring the activity of extracellular and intracellular enzymes derived from wastewater microbial communities. Water research, 155, 115-123.

Table legends

Table 1. Names, usage and abbreviations of the 51 TOrCs analyzed in this study and the statistical differences of their k_{biol} after normalization with ATP.

Table 2. Biological characterization of eight sand filter materials and correlation test between TOrCs removal and biomass indicators. The significance of the Pearson's *r* correlation coefficient was adjusted for multiple comparisons by the bonferroni method.

Figure legends

Figure 1. (a) Average global removal of 51 TOrCs by eight sand filter materials in percentage and molar concentration; (b) ATP concentration in eight sand filter samples; Regression (blue line) for predicting (c) mean global biotransformation rate constants (k_{biol}) and (d) average removal percentage of TOrCs from ATP concentration, gray shadow represents the 95% confidence interval.

Figure 2. (a) Non-normalized and (b) normalized biotransformation rate constants (k_{biol}) of 45 TOrCs by eight sand filter materials. The low ATP concentration in the IFW sand (0.76 pmol/g) made the normalized results appear superimposed. The k_{biol} values were scaled within appropriate range (-2, 2) for better visualization. Clustering used the Manhattan distance metric and Ward's minimum variance method (Ward.D2). Six TOrCs were excluded as they did not fit the first-order kinetics.

Figure 3. Taxonomic composition of eight sand filter materials. (a) Comparison of taxa from microscopy (FISH) vs. 16S amplicon (DADA2) vs. metagenome (METAXA2); (b) Relative abundance of microorganisms at the genus level.

Figure 4. Heatmap showing correlations between biotransformation rate constants (k_{biol}) of 45 TOrCs and (a) 62 genera; green bars represents the genera for which we obtained at least one MAG; (b) 30 significantly differential biotransformation related enzymes between the high biomass and the low biomass group. Cutoff is $p < 0.05$, abs(r) > 0.7, observation > 9. Average clustering was based on Euclidean distances.

Figure 5. Principle component analysis (PCA) of eight sand filter materials based on the differential enzymes identified by DESeq2. Square symbol represents the high biomass group, triangle symbol represents the low biomass group, the remaining samples indicated by circles represent IFW and BWA.

Figure 6. Heatmap showing the completeness of xenobiotics degradation pathways in 37 biotransfromation-correlated MAGs. Pathways are identified by “Reconstruct Pathway” tool in KEGG Mapper. Average clustering was based on Euclidean distances.

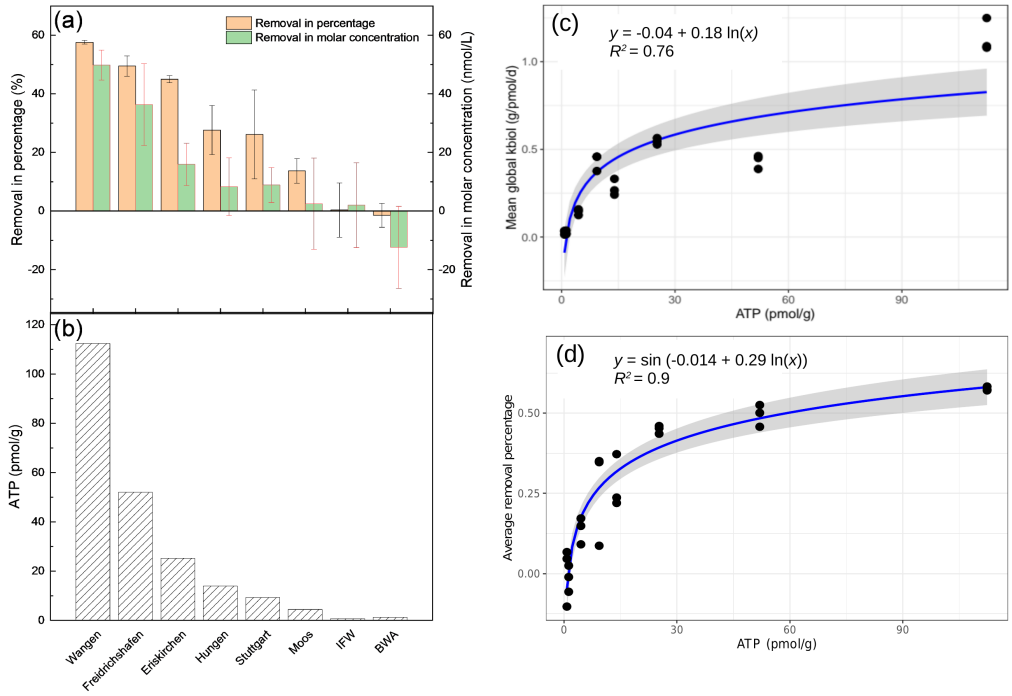

Figure 1. (a) Average global removal of 51 TOrCs by eight sand filter materials in percentage and molar concentration; (b) ATP concentration in eight sand filter samples; Regression (blue line) for predicting (c) mean global biotransformation rate constants (k_{biol}) and (d) average removal percentage of TOrCs from ATP concentration, gray shadow represents the 95% confidence interval.

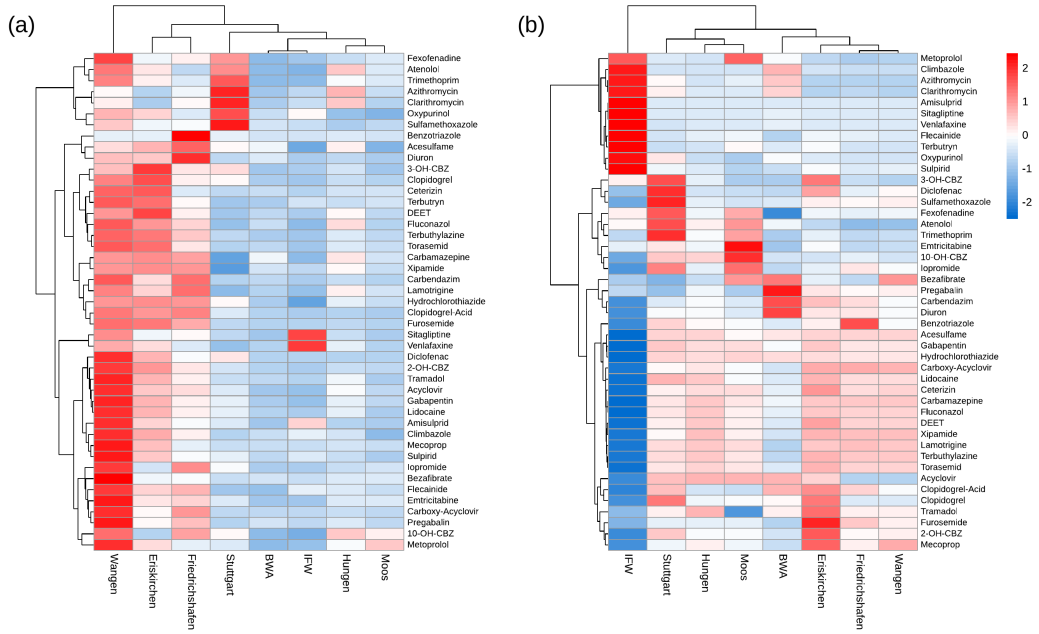

Figure 2. (a) Non-normalized and (b) normalized biotransformation rate constants (k_{biol}) of 45 TOrCs by eight sand filter materials. The low ATP concentration in the IFW sand (0.76 pmol/g) made the normalized results appear superimposed. The k_{biol} values were scaled within appropriate range (-2, 2) for better visualization. Clustering used the Manhattan distance metric and Ward's minimum variance method (Ward.D2). Six TOrCs were excluded as they did not fit the first-order kinetics.

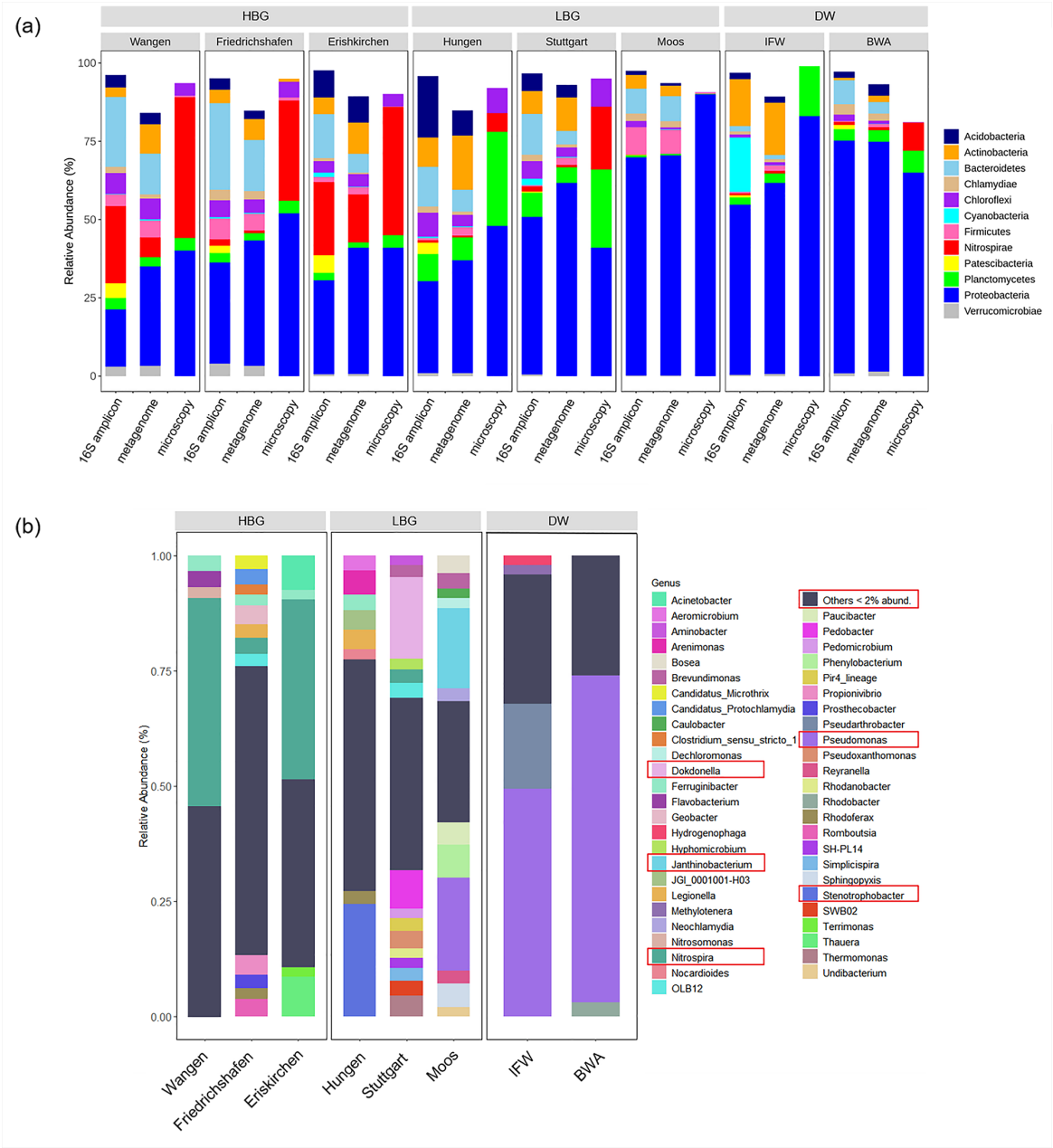

Figure 3. Taxonomic composition of eight sand filter materials. (a) Comparison of taxa from microscopy (FISH) vs. 16S amplicon (DADA2) vs. metagenome (METAXA2); (b) Relative abundance of microorganisms at the genus level.

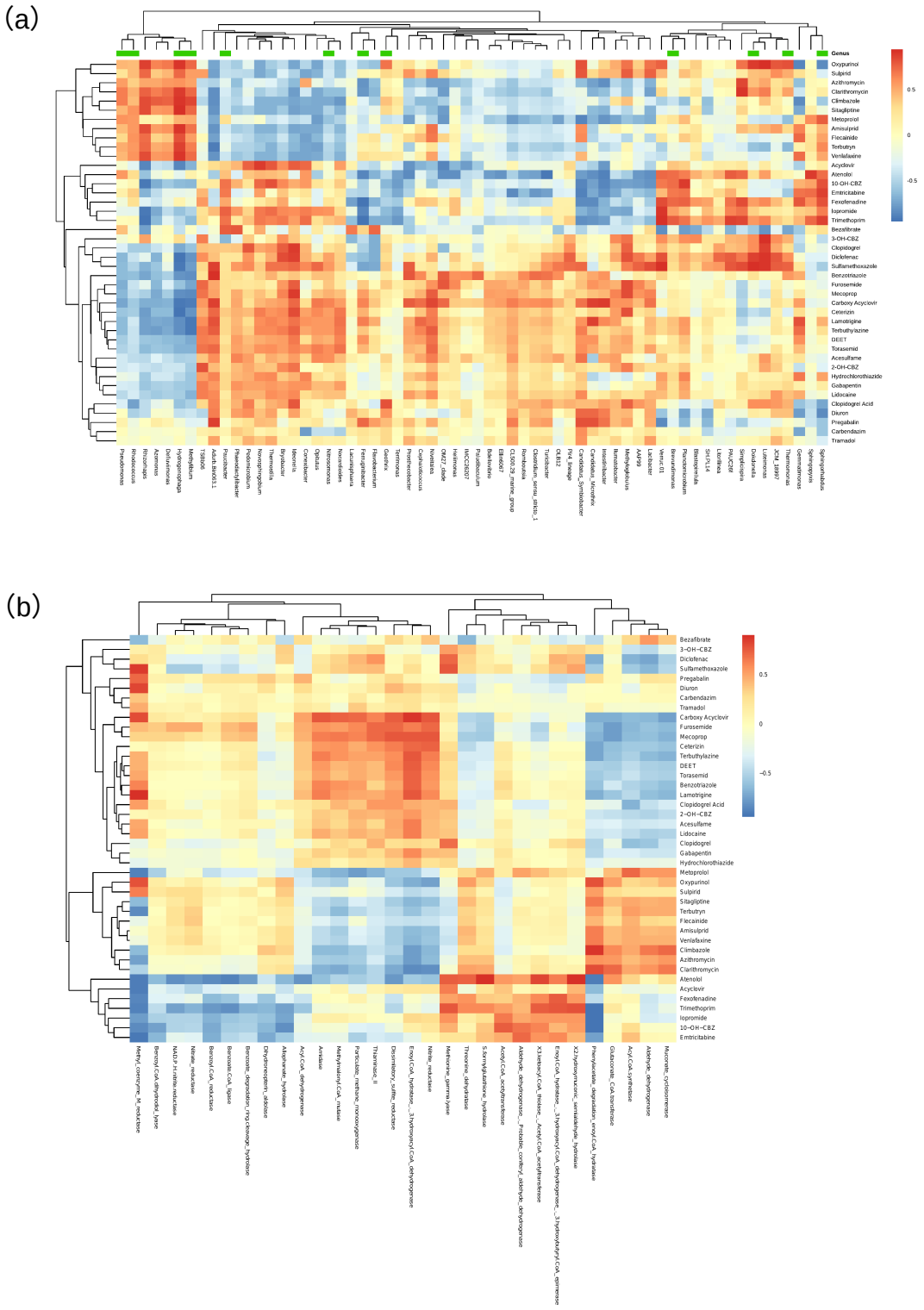

Figure 4. Heatmap showing correlations between biotransformation rate constants (k_{biol}) of 45 TOrCs and (a) 62 genera ; green bars represents the genera for which we obtained at least one MAG; (b) 30 significantly differential biotransformation related enzymes between the high biomass and the low biomass group. Cutoff is $p < 0.05$, abs(r) > 0.7, observation > 9. Average clustering was based on Euclidean distances.

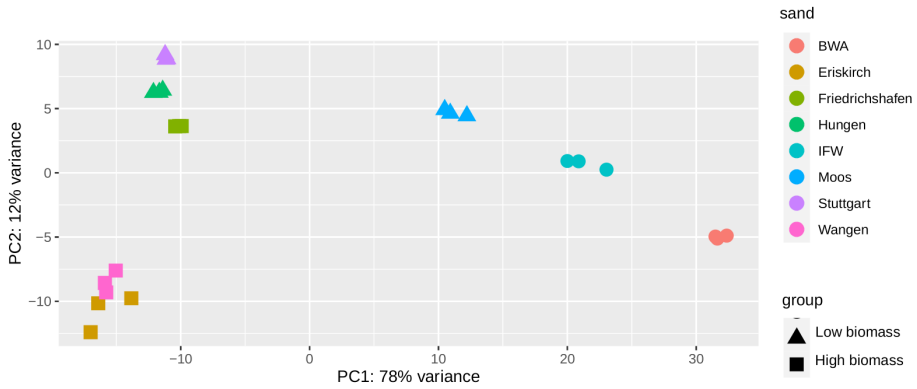

Figure 5. Principle component analysis (PCA) of eight sand filter materials based on the differential enzymes identified by DESeq2. Square symbol represents the high biomass group, triangle symbol represents the low biomass group, the remaining samples indicated by circles represent IFW and BWA.

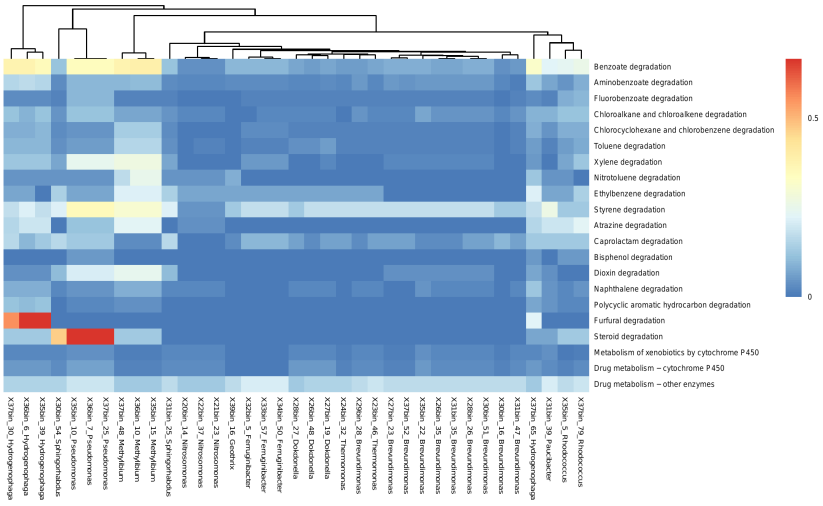

Figure 6. Heatmap showing the completeness of xenobiotics degradation pathways in 37 biotransfromation-correlated MAGs. Pathways are identified by “Reconstruct Pathway” tool in KEGG Mapper. Average clustering was based on Euclidean distances.

Table 1. Names, usage and abbreviations of the 51 TOrCs analyzed in this study and the statistical differences of their k_{biol} after normalization with ATP.

Compound	Usage	Abbreviation	Kruskal-Wallis-Test (adjusted *p*-value)			
			normalizaed		non-normalized	
			between 7 sands	HBG vs LBG	between 7 sands	HBG vs LBG
10-hydroxycarbamazepine	Antiepileptics	10-OH-CBZ	*	**	n.s.	*
2-hydroxycarbamazepine	Antiepileptics	2-OH-CBZ	n.s.	n.s.	**	*
3-hydroxycarbamazepine	Antiepileptics	3-OH-CBZ	*	n.s.	*	*
Acesulfame	Sweetener	ACE	n.s.	n.s.	*	n.s.
Acridone	TP of 10-OH-CBZ	-	-	-	-	-
Acyclovir	Antivirals	ACV	n.s.	*	**	*
Amisulprid	Neuroleptics	-	n.s.	n.s.	**	*
Atenolol	Beta-Blockers	ATN	*	**	n.s.	*
Azithromycin	Antibiotics (macrolides)	AZI	*	**	n.s.	*
Benzotriazole	Industrial	BTA	n.s.	n.s.	*	*
Bezafibrate	Lipid modifying agent	BEZ	n.s.	n.s.	**	*
Caffeine	Psychoactive drug	CAF	-	-	-	-
Carbendazim	Fungicide	-	n.s.	n.s.	**	*
Carboxy-Acyclovir	TP of acyclovir	-	*	*	**	*
Carbamazepine	Antiepileptics	CBZ	n.s.	n.s.	*	n.s.
Ceterizin	Antihistamine	CTZ	n.s.	n.s.	**	*
Clarithromycin	Antibacterials	CLR	*	**	n.s.	*
Climbazole	Antifungal	CZ	*	n.s.	**	*
Clopidogrel acid	Metabolite of clopidogrel	-	*	n.s.	**	*
Clopidogrel	Antiaggregant (pro-drug)	CLO	*	n.s.	**	*
N,N-Diethyl-meta-toluamide	Insecticide/Repellent	DEET	n.s.	n.s.	**	*
Diclofenac	Antiinflammatory	DCF	*	n.s.	*	*
Diuron	Herbicide/Algicide	DIU	*	*	**	*
Emtricitabine	Virostatic agent	EMT	*	*	**	*
Fexofenadine	Antihistamine	FEX	*	*	n.s.	*
Flecainide	Antiarrhythmics	FLEC	n.s.	n.s.	**	*

Fluconazol	Antimycotics	FCZ	n.s.	n.s.	*	n.s.
Furosemide	Loop diuretics	FRM	*	**	**	*
Gabapentin	Anticonvulsant drug	GAP	n.s.	n.s.	**	*
Hydrochlorothiazide	Diuretics	HCT	n.s.	n.s.	*	n.s.
Ibuprofen	Antirheumatic drug	IBU	-	-	-	-
Iopromide	Contrast media	IOP	*	n.s.	*	*
Lamotrigine	Anticonvulsant drug	LTG	n.s.	*	*	n.s.
Levetiracetam acid	TP of levetiracetam	-	-	-	-	-
Lidocaine	Local anaesthetic	LD	n.s.	n.s.	*	*
Mecoprop	Herbicide	MCPP	*	**	**	*
Metoprolol	Beta blockers	MET	n.s.	**	n.s.	*
Oxypurinol	Metabolite of allopurinol (antigout agent)	OP	*	n.s.	n.s.	*
Pregabalin	Anticonvulsant drug	PGB	n.s.	*	**	*
Ramiprilat	Antihypertensives	-	-	-	-	-
Sitagliptine	Antidiabetics	SG	n.s.	n.s.	**	*
Sulfamethoxazole	Antibacterials	SMX	*	n.s.	n.s.	*
Sulpirid	Neuroleptics	SP	n.s.	n.s.	**	*
Terbuthylazine	Herbicide	TBA	n.s.	n.s.	**	*
Terbutryn	Herbicide/Algicide	-	n.s.	n.s.	**	*
Torasemid	Diuretics	-	n.s.	n.s.	**	*
Tramadol	Analgesic	TRA	n.s.	n.s.	*	*
Trimethoprim	Antibacterials	TMP	*	**	n.s.	*
Valsartan	Antihypertensives	VAL	-	-	-	-
Venlafaxine	Psychoanaleptics	VEN	n.s.	n.s.	n.s.	n.s.
Xipamide	Diuretics	XPD	n.s.	n.s.	*	n.s.

TP: transformation products

n.s.: $p \geq 0.05$; *: $0.01 \leq p < 0.05$; **: $0.001 \leq p < 0.01$

Table 2. Biological characterization of eight sand filter materials and correlation test between TOrCs removal and biomass indicators. The significance of the Pearson's *r* correlation coefficient was adjusted for multiple comparisons by the bonferroni method.

Sampling site	Sand filter type	Material	Loss on ignition (mg biomass/g)	ATP (pmol/g)	DNA concentration (ng/g)	Viable cell counts (cells/g)	Dead cell counts (cells/g)	Total cell counts (cells/g)	Alpha diversity	
									Chao1	Inverse Simpson
Hungen	No addition	Quartz gravel	2.23	13.98	1.6	1.58E+08	8.10E+07	8.10E+07	2197.90	105.07
Stuttgart	No addition	Anthracite	13.61	9.34	3.6	9.81E+08	3.79E+08	3.79E+08	993.67	120.87
IFW	Artificial groundwater recharge	Quartz sand	3.40	0.76	1.3	6.27E+07	1.46E+08	1.46E+08	824.76	10.59
BWA	Waterworks	Quartz sand	9.02	1.25	1.9	1.60E+08	1.00E+08	1.00E+08	787.93	8.01
Moos	Precipitant addition	Quartz gravel	2.96	4.48	1.2	2.35E+08	1.34E+08	1.34E+08	826.78	48.31
Friedrichshafen	Precipitant and carbon source addition	Anthracite	314.19	52.00	3.9	1.57E+09	3.30E+08	3.30E+08	2072.95	290.81
Eriskirchen	Precipitant addition	Anthracite	179.46	25.27	3	5.69E+08	2.23E+08	2.23E+08	1357.69	65.54
Wangen	Precipitant addition	Pumice	41.15	112.41	3.2	1.34E+09	2.90E+08	2.90E+08	1069.59	38.19
Non-normalized biotransformation rate constants (k_{biol})	correlation coefficient		0.25	0.92	0.64	0.76	0.61	0.75	0.16	0.15
	adjusted *p*-value		1.00	< 0.001	0.006	< 0.001	0.01	< 0.001	1.00	1.00